Rapid Communications

Route to bursting via pulse-shaped explosion

Xiujing Han,[1,2,3,*] Qinsheng Bi,[1] and Jürgen Kurths[2,3]

[1]*Faculty of Civil Engineering and Mechanics, Jiangsu University, Zhenjiang Jiangsu 212013, People's Republic of China*

[2]*Department of Physics, Humboldt University, Berlin 12489, Germany*

[3]*Potsdam Institute for Climate Impact Research, Potsdam 14473, Germany*

(Received 12 February 2018; revised manuscript received 2 May 2018; published 5 July 2018)

This Rapid Communication reports on the discovery of a route to bursting, called a pulse-shaped explosion (PSE), for a paradigmatic class of nonlinear oscillators. We find that both an equilibrium and a limit cycle can exhibit pulse-shaped sharp quantitative changes in relation to the variation of system parameters, which are interesting explosive behaviors, the PSE. It leads to large-amplitude oscillations in the rest phase (i.e., small-amplitude oscillations) of bursting, giving rise to additional active phases alternating with the rest phase, and finally determines compound bursting structures. This way, the route to complex bursting dynamics by PSE is explained and its robustness is shown. PSE opens different ways for the control dynamics of complex systems.

DOI: 10.1103/PhysRevE.98.010201

As a representative of complex, multiple-timescale dynamics, bursting has received much attention in the past several decades. Typically, bursting contains small-amplitude oscillations (i.e., the rest phase of bursting) which alternate with large-amplitude oscillations (i.e., the active phase of bursting) [1]. Such a complex oscillation mode is frequently observed in neuronal systems [2–4], biological signal transduction [5,6], calcium dynamics [7,8], and other fields [9–11]. Regarding the dynamical mechanisms of bursting, it has been demonstrated that bursting is often linked to sharp transitions of dynamical systems. For example, based on the fast-slow analysis [12], it has been found that a system's activity can alternate between different phases via canard phenomena [13,14], the blue-sky catastrophe [15,16], delayed bifurcations [17,18] and other fast transitions related to hard bifurcations [1,11,19], and hence bursting.

Recently, another sharp transition behavior, called the speed escape of attractors [20], was uncovered based on nonlinear oscillators of Rayleigh's type [21–23]. This transition leads attractors to infinity in a narrow parameter interval near the critical escape (CE) line. Because the narrow parameter interval witnesses a sharp transition of attractors, it forms an active area of bursting, which has been identified as playing decisive roles in the generation of bursting. The resultant bursting patterns, however, often show simple dynamical characteristics. In the present Rapid Communication, in order to describe compound bursting dynamics in nonlinear oscillators of Rayleigh's type, we propose a sharp transition behavior, called a pulse-shaped explosion (PSE), which is characterized by pulse-shaped sharp quantitative changes appearing in the branches of the equilibrium point and limit cycle. We explain the generation of PSE based on fold bifurcations of the CE transitions. In particular, we show that it is the PSE that complicates bursting dynamics and finally determines compound bursting structures (Fig. 1).

To describe our results, we extend the paradigmatic externally and parametrically excited Rayleigh oscillator with 1 : 2 frequency ratios [22] to the one with $1:n$ frequency ratios. Then, the following extended Rayleigh oscillator is obtained,

$$\ddot{x} + f(\dot{x}) + [1 - \mu\cos(n\omega t)](x + \gamma x^3) = q\cos(\omega t), \quad (1)$$

where $f(\dot{x}) = -\alpha\dot{x} + \beta\dot{x}^3$ is the Rayleigh's nonlinear function and $\mu\cos(n\omega t)$ and $q\cos(\omega t)$ are two excitations. In order to facilitate the analysis, throughout this Rapid Communication, the parameters β, γ, and q are fixed at the same values as in Ref. [20] (see Fig. 1), while α is a control parameter, related to the transition between an equilibrium and a limit cycle. For this case, the natural frequency of the system can be an $O(1)$ quantity. Furthermore, we assume that ω ($\omega \ll 1$) is small enough so that the two excitations vary slowly and that there is a gap between the natural frequency of the system and the frequencies of the excitations. Then, system (1) becomes a fast-slow system with two slow variables (i.e., the two slow excitations), and the transformed fast-slow analysis given in Ref. [24] allows us to investigate the bursting dynamics of the system.

Compared to the same system with $n = 2$ in which a relatively simple bursting dynamics is observed (Fig. 2), system (1) with $n \geqslant 3$ exhibits a large amount of complex bursting patterns showing compound structures (Fig. 1), characterized by multiple clusters that can be observed in each cycle of the bursting. These compound bursting structures can be divided into two classes according to the PSE related to different types of attractors, which will be explored later.

According to our method given in Ref. [24], system (1) can be transformed into a fast-slow form with one single slow variable. The slow variable is $y(t) = \cos(\omega t)$ and the fast subsystem is given by

$$\ddot{x} + f(\dot{x}) + [1 - \mu g_n(\delta)](x + \gamma x^3) = q\delta, \quad (2)$$

where $\delta = y$ is the control parameter and $g_n(x)$ is the corresponding trigonometric polynomial for $\cos(n\omega t)$, i.e., $g_n(x) = C_n^0 x^n - C_n^2 x^{n-2}(1-x^2) + C_n^4 x^{n-4}(1-x^2)^2 - \cdots + i^m C_n^m x^{n-m}(1-x^2)^{\frac{m}{2}}$, where i is the imaginary unit and m is the maximum even number not larger than n.

*xjhan@mail.ujs.edu.cn

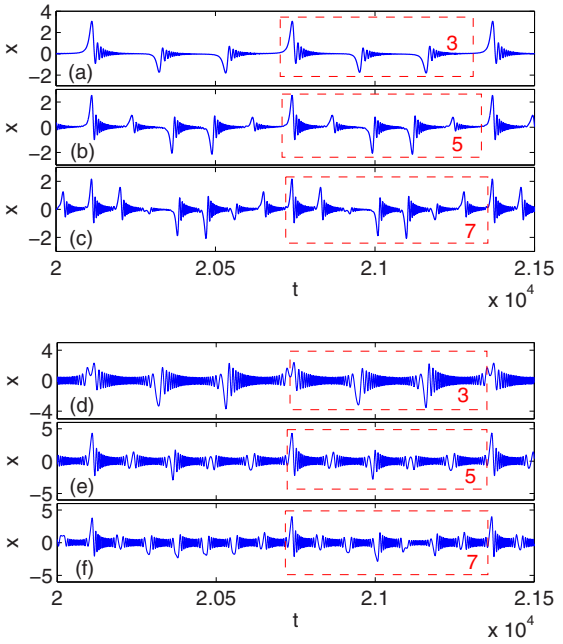

FIG. 1. Typical examples of PSE-induced compound bursting structures in system (1). (a) $n = 3$ and $\alpha = -0.05$; (b) $n = 5$ and $\alpha = -0.05$; (c) $n = 7$ and $\alpha = -0.05$; (d) $n = 3$ and $\alpha = 0.02$; (e) $n = 5$ and $\alpha = 0.02$; (f) $n = 7$ and $\alpha = 0.02$. The other parameters are fixed at $\beta = 0.05$, $\mu = 0.99$, $\omega = 0.01$, $\gamma = 0.1$, and $q = 0.05$. The red numbers 3, 5, and 7 indicate the number of clusters in each period of bursting.

If $1 - \mu g_n(\delta) \neq 0$, the fast subsystem has one single equilibrium, written in the form $(x,0)$, where x is decided by the real root of $[\mu g_n(\delta) - 1](x + \gamma x^3) + q\delta = 0$. The equilibrium will approach infinity as μ and δ approach the CE transition condition $1 - \mu g_n(\delta) = 0$, i.e., $\mu = \frac{1}{g_n(\delta)}$, at which no equilibrium exists.

Based on this transition condition, we next explore the PSE related to the equilibrium. In order to provide a clear understanding of this phenomenon, we first discuss a simple PSE showing one single peak. This is related to the case $n = 3$. Figure 3(a) shows a bifurcation behavior of the fast subsystem for fixed $\alpha = -0.05$. We find that the number of CE curves varies with μ. In particular, two CE lines, CE_f and CE3, are observed at the critical value $\mu_f = 1$ [Fig. 3(b)], where a fold bifurcation related to CE transitions takes place, i.e., a small perturbation of μ leads CE_f to disappear or to split into CE1 and CE2.

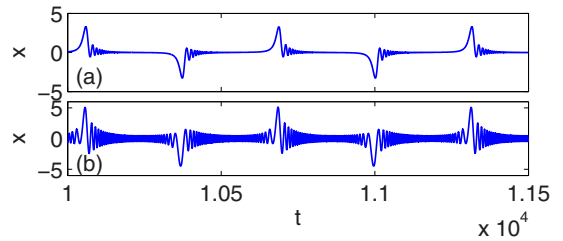

FIG. 2. Typical bursting patterns in system (1) with $n = 2$. (a) $\alpha = -0.05$; (b) $\alpha = 0.02$. The other parameters are the same as in Fig. 1.

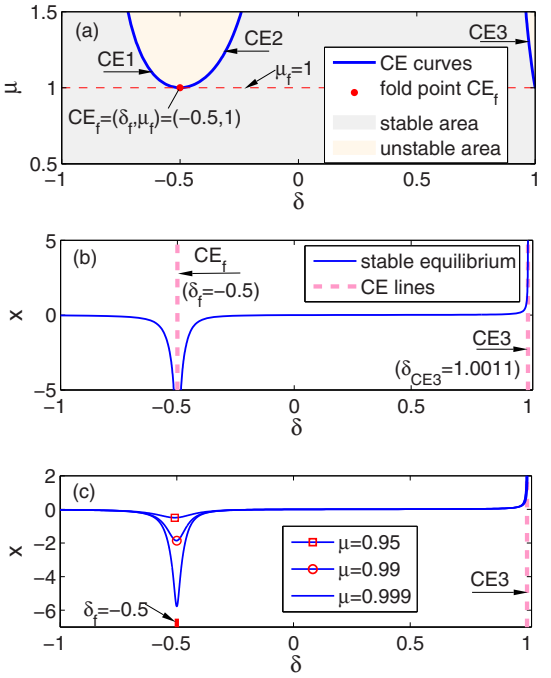

FIG. 3. Disappearance of CE transitions by a fold bifurcation (a), (b) leads to PSE of the equilibrium, the peak of which is sharply decreased as μ decreases (c). (a) CE curves in the parameter plane (δ,μ), where a fold point CE_f is observed at $(\delta_f,\mu_f) = (-0.5,1)$. (b) Critical bifurcation behavior for $\mu = \mu_f = 1$. (c) An evolution of PSE. The above are simulations related to the fast subsystem (2) for fixed $\alpha = -0.05$ and $n = 3$.

Here, we focus on the sharp transitions near the critical line CE_f. As shown in Fig. 3(b), on each side of the CE_f line there is a stable equilibrium branch, which becomes extremely steep when sticking closely to CE_f and approaches infinity as $\delta \to \delta_f$ ($\delta_f = -0.5$). When CE_f disappears, the two originally disunited steep branches now inosculate as a whole. As a result, a complete stable equilibrium branch, which inherits the "steep" properties from the originally disunited branches, is created. Such "steep" properties form pulse-shaped sharp quantitative changes in relation to the variation of δ near δ_f [see Fig. 3(c)]. We call this observed sharp transition a PSE.

An evolution of the PSE is shown in Fig. 3(c). It is seen that the peak is sharply decreased as μ decreases, and finally disappears when μ decreases to some value. From another point of view, a spike will appear in the flat equilibrium curve as μ increases and approaches μ_f, and finally is split into two extremely steep branches stretching into infinity when μ increases to μ_f.

Complex PSEs showing two or multiple peaks can be observed in the fast subsystem for $n > 3$. For $n = 5$, Fig. 4(a) shows two fold points of CE curves for fixed $\alpha = -0.05$. Note that a fold point indicates a peak in the equilibrium curve. Therefore, in this case, two peaks are created [Fig. 4(b)]. For $n = 7$, three fold points are observed for fixed $\alpha = -0.05$, which thus lead to three peaks in the equilibrium curve [Figs. 4(c) and 4(d)].

Now we turn to a consideration of PSE related to a limit cycle. We focus on the critical bifurcation behavior in Fig. 3(b)

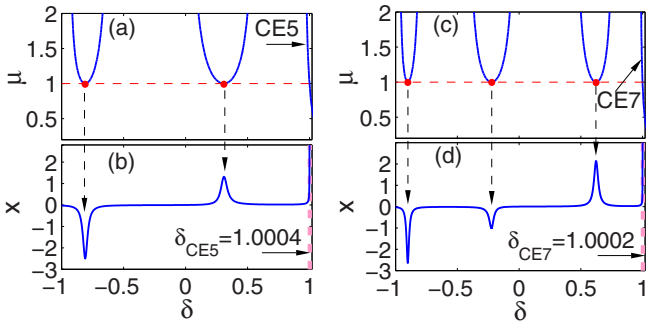

FIG. 4. Fold points in the parameter plane (δ,μ) (a), (c) and the resultant PSEs showing peaks whose numbers are the same as those of the fold points (b), (d). In (a), (c), the μ coordinate of fold points are $\mu_f = 1$. In (b), (d), $\mu = 0.99$. (a), (b) are simulations related to the fast subsystem (2) for fixed $\alpha = -0.05$ and $n = 5$, while (c), (d) for fixed $\alpha = -0.05$ and $n = 7$.

and let the control parameter α increase from -0.05. It is easy to check that, when α increases through $\alpha_H = 0$, the stable equilibrium branches lose their stabilities by a supercritical Hopf bifurcation, and meanwhile a branch of a limit cycle attractor is created on both sides of CE_f [see Fig. 5(a)]. For this case, the line CE_f now indicates CE transitions related to unstable equilibrium. Note that the limit cycle attractor, which can be identified typically in terms of its period and maximum of some variable if δ is a fixed parameter, surrounds the unstable equilibrium all the time, and thus undergoes a sharp transition along with it. That is, as the disappearance of CE_f, the PSE related to a limit cycle attractor will appear [see Fig. 5(b)].

A similar rapid recession of the peak is observed for the PSE related to a limit cycle attractor [see Fig. 5(b)]. Besides, complex PSEs related to a limit cycle attractor can also be observed as long as α is increased such that the equilibrium branch showing two or multiple peaks loses its stability by a supercritical Hopf bifurcation (see Fig. 6).

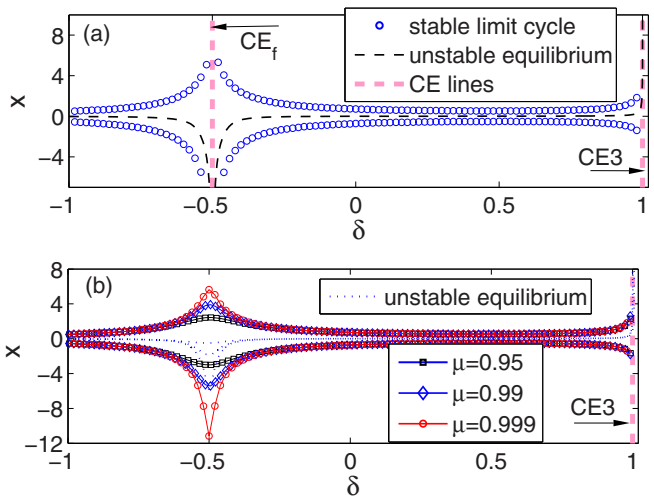

FIG. 5. PSE of a stable limit cycle comes into being with the PSE of unstable equilibrium. (a) Critical bifurcation behavior, in which $\alpha = 0.02$ and the other parameters are the same as in Fig. 3(b). (b) An evolution of the PSE of stable limit cycle, where $\alpha = 0.02$ and the other parameters are the same as in Fig. 3(c).

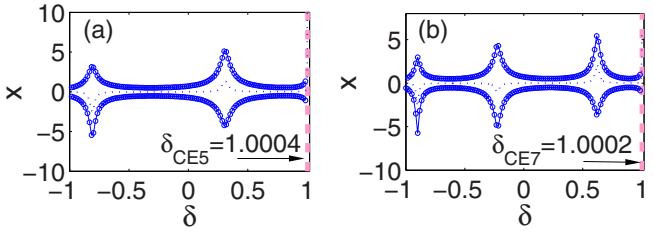

FIG. 6. Complex PSEs related to a limit cycle attractor, showing two (a) and multiple (b) peaks. Here, α is fixed at $\alpha = 0.02$, and the other parameters in (a) and (b) are the same as in Figs. 4(b) and 4(d), respectively.

Based on the PSEs revealed above, in what follows we explore the generation of compound bursting dynamics. Figure 7 shows rest areas and active areas for bursting based on the stable equilibrium curve $\mu = 0.99$ in Fig. 3(c). Obviously, without PSE, the curve can be divided into two parts: a steep part which indicates an active area for bursting and a flat part which means a rest area for bursting. Note that the PSE essentially means sharp transitions. Therefore, an additional active area A_p, induced by the PSE, exists near δ_f. When the slow variable $\cos(\omega t)$ is "switched on," a bursting trajectory periodically passes through A_p, leading to two additional sharp transitions in each period of bursting. As a result, two additional clusters related to the PSE appear in bursting, which thus complicates the bursting dynamics and creates a compound bursting structure [see Fig. 8(a)]. In particular, more peaks in the stable equilibrium branch indicate more active areas for bursting, which is the reason for the generation of more complex compound bursting structures [see Figs. 8(b) and 8(c)].

Similarly, one may conclude that the above results are also true for the case when the PSE is related to a limit cycle attractor [e.g., see Fig. 8(d)]. This is exactly the reason for the generation of compound bursting structures as shown in Figs. 1(d)–1(f).

In summary, we have reported the existence of PSE, a kind of sharp transition related to an equilibrium and a limit cycle. Typically, extremely steep solution branches can be observed near CE transition lines. Our study shows that the two steep solution branches can inosculate as a whole by a fold bifurcation of CE transitions. In particular, the resulting whole solution branch remains the steep characteristics near the critical CE lines related to fold points of CE transitions.

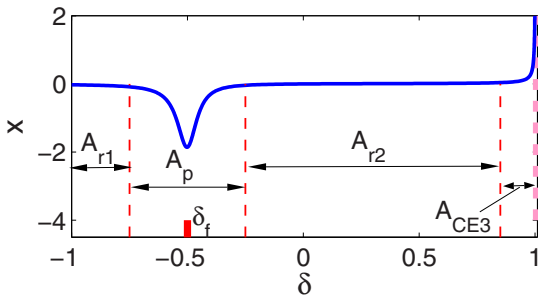

FIG. 7. Schematic diagram: Various areas formed by different dynamical characteristics of the equilibrium curve with $\mu = 0.99$ in Fig. 3(c). A_{r1} and A_{r2} are rest areas, A_p is the active area induced by PSE, and A_{CE3} denotes the active area related to the CE3 transition.

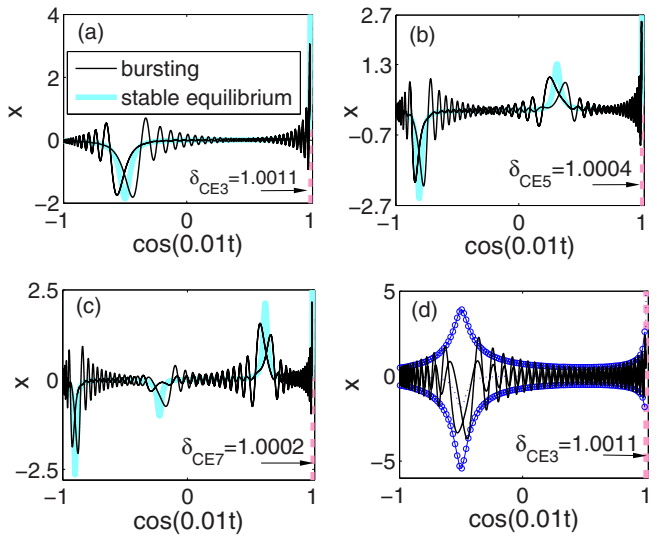

FIG. 8. Fast-slow analysis of the compound bursting structures in Figs. 1(a)–1(d). The values of $\delta_{CE3,5,7}$ indicate that, near $\delta = 1$, there is a CE-transition-induced active area for the bursting.

This thus leads to pulse-shaped sharp quantitative changes in the solution branch and therein lies the generation of PSE. PSE creates additional active areas for bursting and increases the number of clusters in bursting. Based on this, an interesting route to complex bursting dynamics is presented.

Here, our analysis focuses on typical examples of bursting patterns related to odd values of n. The PSE and the compound bursting structures can also be observed if n is even. In particular, larger n often means more PSEs, which thus lead to a cluster adding effect. Note that such an effect is related to a fixed bursting period (Figs. 1 and 8), and thus it is quite different compared to the period adding cascade phenomenon [19,25,26], a typical dynamical mechanism complicating bursting dynamics. Further analysis shows that interesting behaviors related to the period of the limit cycle and the complex eigenvalues for the equilibrium are observed near PSE, e.g., all of these related quantities reach an extreme value near PSE (e.g., see Fig. 9). How this relates to the PSE is an interesting problem and needs further investigation.

Besides, our analysis is based on a specific Rayleigh oscillator. However, because the Rayleigh oscillator in its various forms can be used to approximately describe many physical phenomena and processes in mechanical and electrical engineering [21–23,27], and because there are significant

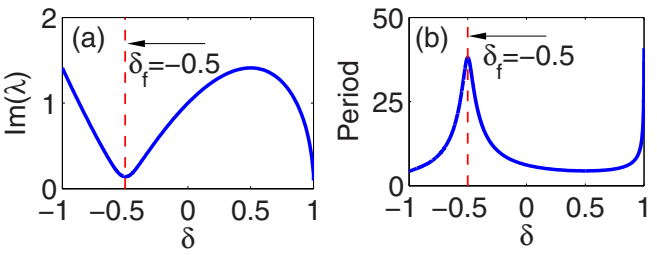

FIG. 9. Imaginary part of the eigenvalues (a) for the equilibrium branch in Fig. 8(a) and the period (b) of the branch of limit cycle attractor in Fig. 8(d).

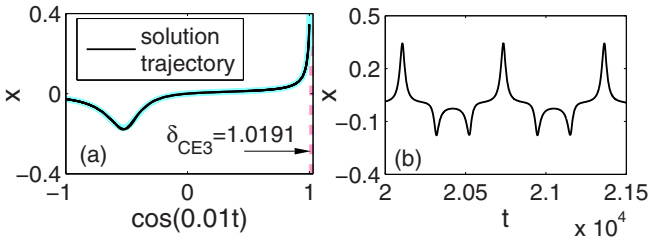

FIG. 10. Sharp transitions cannot be created if the peak is not large enough. For this case, the solution trajectory follows the stable equilibrium obediently without sharp transitions (a), and thus a compound bursting structure cannot be obtained; instead, a relatively simple oscillatory mode is created (b). Here, $\mu = 0.85$, and the other parameters are the same as in Fig. 8(a).

numbers of hybrid systems related to nonlinear oscillators of Rayleigh's type, e.g., Rayleigh-Duffing oscillators [28] and Rayleigh–van der Pol oscillators [29], the proposed PSE and the resultant compound bursting structures should be observed in various related dynamical systems as well as in experiments.

The PSE itself exhibits interesting dynamical characteristics. We have shown that, after the disappearance of CE transitions by fold bifurcations, the peak of PSE will decrease and finally goes almost to zero. Surely, there is a critical peak for complex bursting dynamics, and only when the peak is larger than such a critical value, we observe sharp transitions that compound bursting structures rely on (Fig. 10). However, how large the critical peak is remains hazy and needs to be further explored.

Below the critical peak, the attractor previously showing a PSE will turn into a common one. That is, PSE is in a transition phase from the disappearance of sharp CE transitions to the appearance of mild dynamical behavior. Note that PSE is a typical kind of sharp transition behavior. Therefore, such a transition phase in fact extends the parameter range showing sharp transitions near the fold point, and this may bring about new problems for the study of stability and control of dynamical systems.

Finally, we would like to point out that PSE has shown the existence of an amplitude-modulated limit cycle attractor, i.e., a periodic attractor whose amplitude shows to-and-fro varyings as the system parameters vary (see Fig. 6). On the other hand, as noted earlier, if the peaks that the amplitude-modulated limit cycle attractor exhibits are smaller than some critical peak, the solution trajectory will follow the attractor closely without sharp transitions, i.e., amplitude-modulated oscillations will appear. Therefore, amplitude-modulated bursting [8], a class of bursting reported recently, may be generated if an amplitude-modulated limit cycle attractor with small peaks becomes the active state of bursting. That is, an amplitude-modulated limit cycle attractor with small peaks forms a possible mechanism underlying the appearance of amplitude-modulated bursting. Based on this, we conclude that the proposed PSE can help to explore the diversity of dynamical mechanisms of specific bursting patterns.

The authors express their gratitude to the anonymous reviewers whose comments and suggestions have helped improve this manuscript. This work is supported by the

National Natural Science Foundation of China (Grants No. 11572141, No. 11632008, No. 11772161, and No. 11502091) and the Training Project for Young Backbone Teacher of Jiangsu University.

[1] E. M. Izhikevich, Int. J. Bifurcation Chaos **10**, 1171 (2000).
[2] G. S. Medvedev, Phys. Rev. Lett. **97**, 048102 (2006).
[3] P. Channell, G. Cymbalyuk, and A. Shilnikov, Phys. Rev. Lett. **98**, 134101 (2007).
[4] T. S. Okubo, E. L. Mackevicius, H. L. Payne, G. F. Lynch, and M. S. Fee, Nature (London) **528**, 352 (2015).
[5] S. M. Bezrukov and I. Vodyanoy, Nature (London) **378**, 362 (1995).
[6] E. M. Izhikevich, N. S. Desai, E. C. Walcott, and F. C. Hoppensteadt, Trends Neurosci. **26**, 161 (2003).
[7] R. Larter and M. G. Craig, Chaos **15**, 047511 (2005).
[8] T. Vo, M. A. Kramer, and T. J. Kaper, Phys. Rev. Lett. **117**, 268101 (2016).
[9] T. Hayashi, Phys. Rev. Lett. **84**, 3334 (2000).
[10] D. X. Tran, D. Sato, A. Yochelis, J. N. Weiss, A. Garfinkel, and Z. L. Qu, Phys. Rev. Lett. **102**, 258103 (2009).
[11] C. Kuehn, *Multiple Time Scale Dynamics* (Springer, Berlin, 2015).
[12] J. Rinzel, in *Ordinary and Partial Differential Equations*, edited by B. D. Sleeman and R. J. Jarvis (Springer, Berlin, 1985), pp. 304–316.
[13] P. Szmolyan and M. Wechselberger, J. Differ. Equations **177**, 419 (2001).
[14] M. Krupa, A. Vidal, M. Desroches, and F. Clément, SIAM J. Appl. Dyn. Syst. **11**, 1458 (2012).
[15] A. Shilnikov and G. Cymbalyuk, Phys. Rev. Lett. **94**, 048101 (2005).
[16] A. L. Shilnikov, L. P. Shilnikov, and D. V. Turaev, Moscow Math. J. **5**, 269 (2005).
[17] S. M. Baer, T. Erneux, and J. Rinzel, SIAM J. Appl. Math. **49**, 55 (1989).
[18] X. J. Han, Q. S. Bi, C. Zhang, and Y. Yu, Int. J. Bifurcation Chaos **24**, 1450098 (2014).
[19] M. Desroches, J. Guckenheimer, B. Krauskopf, C. Kuehn, H. M. Osinga, and M. Wechselberger, SIAM Rev. **54**, 211 (2012).
[20] X. J. Han, F. B. Xia, C. Zhang, and Y. Yu, Nonlinear Dyn. **88**, 2693 (2017).
[21] K. Szabelski and J. Warmiński, Int. J. Nonlinear Mech. **30**, 179 (1995).
[22] J. Warminski, Nonlinear Dyn. **61**, 677 (2010).
[23] L. Cveticanin, in *Proceedings of the 14th IFToMM World Congress 14th-6, Taipei* (IFToMM, 2015), pp. 93–100.
[24] X. J. Han, Q. S. Bi, P. Ji, and J. Kurths, Phys. Rev. E **92**, 012911 (2015).
[25] M. Brøns, T. J. Kaper, and H. G. Rotstein, Chaos **18**, 015101 (2008).
[26] E. J. Doedel, B. E. Oldeman, and C. L. Pando L., Int. J. Bifurcation Chaos **21**, 305 (2011).
[27] H. Hasegawa, Phys. Rev. E **84**, 061112 (2011).
[28] Y. Kanai and H. Yabuno, Nonlinear Dyn. **70**, 1007 (2012).
[29] S. Erlicher, A. Trovato, and P. Argoul, Mech. Syst. Signal Process. **41**, 485 (2013).